



## Article

# Role of IRE1 $\alpha$ /XBP1/CHOP/NLRP3 Signalling Pathway in Neonicotinoid Imidacloprid-Induced Pancreatic Dysfunction in Rats and Antagonism of Lycopene: In Vivo and Molecular Docking Simulation Approaches

Walaa Bayoumie El Gazzar <sup>1,2</sup>, Heba Bayoumi <sup>3</sup>, Heba S. Youssef <sup>4</sup> , Tayseer A. Ibrahim <sup>4</sup> ,  
Reham M. Abdelfatah <sup>5</sup> , Noha M. Gamil <sup>6</sup> , Mervat K. Iskandar <sup>7</sup>, Amal M. Abdel-Kareim <sup>7</sup>,  
Shaymaa M. Abdelrahman <sup>2</sup>, Mohammed A. Gebba <sup>8</sup>, Mona Atya Mohamed <sup>3</sup>, Maha M. Mokhtar <sup>9</sup>,  
Tayseir G. Kharboush <sup>10</sup>, Nervana M. Bayoumy <sup>11</sup> , Hatun A. Alomar <sup>12</sup>  and Amina A. Farag <sup>9,\*</sup> 

- <sup>1</sup> Department of Anatomy, Physiology and Biochemistry, Faculty of Medicine, The Hashemite University, P.O. Box 330127, Zarqa 13133, Jordan; wallagazzar@hu.edu.jo
  - <sup>2</sup> Department of Medical Biochemistry & Molecular Biology, Faculty of Medicine, Benha University, Benha 13518, Egypt; shaimaa.bghdadi@fmed.bu.edu.eg
  - <sup>3</sup> Department of Histology and Cell Biology, Faculty of Medicine, Benha University, Benha 13518, Egypt; heba.bayoumi@fmed.bu.edu.eg (H.B.); mona.fady@fmed.bu.edu.eg (M.A.M.)
  - <sup>4</sup> Department of Physiology, Faculty of Medicine, Benha University, Benha 13518, Egypt; heba.youssef@fmed.bu.edu.eg (H.S.Y.); tayseer.alaa@fmed.bu.edu.eg (T.A.I.)
  - <sup>5</sup> Department of Pesticides, Faculty of Agriculture, Mansoura University, Mansoura 35516, Egypt; reham\_2010@mans.edu.eg
  - <sup>6</sup> Department of Pharmacology and Toxicology, Faculty of Pharmaceutical Sciences and Drug Manufacturing, Misr University for Science and Technology, 6th of October City 12573, Egypt; noha.mohsen@must.edu.eg
  - <sup>7</sup> Department of Zoology, Faculty of Science, Benha University, Benha 13518, Egypt; mervat.iskandar@fsc.bu.edu.eg (M.K.I.); amel.abdelkarim@fsc.bu.edu.eg (A.M.A.-K.)
  - <sup>8</sup> Department of Anatomy & Embryology, Faculty of Medicine, Benha University, Benha 13518, Egypt; mohamed.gaba@fmed.bu.edu.eg or mohammedgebba@gmail.com
  - <sup>9</sup> Department of Forensic Medicine and Clinical Toxicology, Faculty of Medicine, Benha University, Benha 13518, Egypt; maha.mahmoud@fmed.bu.edu.eg
  - <sup>10</sup> Department of Pharmacology and Therapeutics, Faculty of Medicine, Benha University, Benha 13518, Egypt; tyseerg40@gmail.com
  - <sup>11</sup> Department of Physiology, College of Medicine, King Saud University, Riyadh 11461, Saudi Arabia; nbayoumy@ksu.edu.sa
  - <sup>12</sup> Pharmacology and Toxicology Department, Faculty of Pharmacy, King Saud University, Riyadh 11451, Saudi Arabia; hetalamar@ksu.edu.sa
- \* Correspondence: amina.farag@fmed.bu.edu.eg



**Citation:** El Gazzar, W.B.; Bayoumi, H.; Youssef, H.S.; Ibrahim, T.A.; Abdelfatah, R.M.; Gamil, N.M.; Iskandar, M.K.; Abdel-Kareim, A.M.; Abdelrahman, S.M.; Gebba, M.A.; et al. Role of IRE1 $\alpha$ /XBP1/CHOP/NLRP3 Signalling Pathway in Neonicotinoid Imidacloprid-Induced Pancreatic Dysfunction in Rats and Antagonism of Lycopene: In Vivo and Molecular Docking Simulation Approaches. *Toxics* **2024**, *12*, 445. <https://doi.org/10.3390/toxics12070445>

Academic Editor: José Luis Rodríguez Gutiérrez

Received: 27 April 2024

Revised: 17 June 2024

Accepted: 18 June 2024

Published: 21 June 2024



**Copyright:** © 2024 by the authors. Licensee MDPI, Basel, Switzerland. This article is an open access article distributed under the terms and conditions of the Creative Commons Attribution (CC BY) license (<https://creativecommons.org/licenses/by/4.0/>).

**Abstract:** Imidacloprid (IMI) is a commonly used new-generation pesticide that has numerous harmful effects on non-targeted organisms, including animals. This study analysed both the adverse effects on the pancreas following oral consumption of imidacloprid neonicotinoids (45 mg/kg daily for 30 days) and the potential protective effects of lycopene (LYC) administration (10 mg/kg/day for 30 days) with IMI exposure in male Sprague–Dawley rats. The apoptotic, pyroptotic, inflammatory, oxidative stress, and endoplasmic reticulum stress biomarkers were evaluated, along with the histopathological alterations. Upon IMI administration, noticeable changes were observed in pancreatic histopathology. Additionally, elevated oxidative/endoplasmic reticulum-associated stress biomarkers, inflammatory, pyroptotic, and apoptotic biomarkers were also observed following IMI administration. LYC effectively reversed these alterations by reducing oxidative stress markers (e.g., MDA) and enhancing antioxidant enzymes (SOD, CAT). It downregulated ER stress markers (IRE1 $\alpha$ , XBP1, CHOP), decreased pro-inflammatory cytokines (TNF- $\alpha$ , IL-1 $\beta$ ), and suppressed pyroptotic (NLRP3, caspase-1) along with apoptotic markers (Bax, cleaved caspase-3). It also improved the histopathological and ultrastructure alterations brought on by IMI toxicity.

**Keywords:** imidacloprid; lycopene; endoplasmic reticulum stress; apoptosis; pyroptosis; pancreas

## 1. Introduction

Numerous xenobiotics pose serious risks to both people and the environment. The most prevalent pollutants, pesticides, affect biological structures in both acute and chronic exposures in various ways [1]. Over the past few decades, neonicotinoid pesticides have experienced the fastest rate of growth [2]. Neonicotinoids are frequently used due to their high toxicity to invertebrates, simplicity, versatility, long-lasting effects, and systemic distribution throughout the target crop [3]. However, these characteristics increase the risk of environmental contamination and adverse health effects on exposed organisms. These substances are widely distributed throughout the ecosystem [4], making it easier to encounter toxic levels through inhalation, skin contact, and ingestion of contaminated produce and water [2,5]. IMI is a new-generation pesticide suggested as a safer alternative [4], but its extensive use has been associated with various side effects on non-targeted species [3]. Zhao et al., who reported the presence of IMI and its metabolites in urine samples of the general population, demonstrated this [2,4]. Accumulating research on mammals, chicken embryos, and honey bees suggests that IMI, in addition to causing gastrointestinal insults and neurological symptoms, leads to renal damage, as indicated by increased activity of glutamate pyruvate transaminase and glutamate oxalacetate transaminase, elevated glucose and blood urea nitrogen content, cardiovascular insults, haematological impairments, renal and reproductive organ damage, and hepatotoxicity, reflected in increased bilirubin levels and alterations in liver tissue [3–5]. Recently, IMI's toxic effects on the pancreas have been observed. Findings suggest that IMI may contribute to type 2 diabetes mellitus (T2DM), one of the major metabolic disorders characterized by pancreatic  $\beta$ -cell dysfunction. In addition to one of the diabetogenic pesticides [1], we focus on the pancreas, an organ highly susceptible to oxidative stress and inflammation, particularly inflammatory mediators that affect vascular permeability (e.g., TNF- $\alpha$ , IL-1 $\beta$ , and IL-6) [6], resulting in acinar and  $\beta$  cell dysfunction [7].

According to Karpińska and Czauderna (2022), emerging pancreatic insufficiency is the result of damage to the exocrine region of the pancreas, which causes the pancreas to be unable to biosynthesize and/or produce enough digestive enzymes for the intestines to process and absorb food parts. In addition, diabetes mellitus and its consequences on varied systems of the body develop from beta cell damage [2,3].

Various studies have suggested that the main mechanism of IMI toxicity is oxidative stress combined with inflammation [6,8]. Recent experiments have shown that the NOD-like receptor family pyrin domain-containing 3 (NLRP3) inflammasome plays a crucial role in linking  $\beta$  cell dysfunction and inflammation through its pyroptotic function, which leads to cellular swelling, plasma membrane rupture, and secretion of interleukin (IL)-1 $\beta$  [9]. Although IMI has been observed to induce cellular inflammation, the specific mechanism of IMI-induced pancreatic pyroptosis remains unclear. Tumour necrosis factor alpha (TNF- $\alpha$ ) is a vital component in stimulating the NLRP3 inflammasome, and studies have demonstrated its significant exacerbation by IMI-induced oxidative stress [10–12]. TNF- $\alpha$  is also necessary for the activation of caspase-1 [13]. Currently, there is limited understanding of the mechanism underlying IMI-induced TNF- $\alpha$ -associated cellular damage, and thus, further research is needed to determine whether TNF- $\alpha$  mediates IMI-induced inflammasome production and pyroptosis.

In the presence of abnormally folded or unfolded proteins, the endoplasmic reticulum (ER) directs these proteins to the cytoplasm, where they are eliminated via an ER-associated degradation process (ERAD) [4]. However, in states like inflammation and oxidative stress, the ER may not be able to cope with the levels of damaged proteins, thus triggering ER stress and the unfolded protein response (UPR), which in turn activates the NLRP3 inflammasome, causing cell pyroptosis [4–6,8]. This process has been associated with

neurodegenerative, cardiovascular, and metabolic diseases, such as diabetes mellitus. Although a few studies have demonstrated an association between increased ER stress and IMI exposure, the relationship remains unclear and requires further investigation to comprehensively understand the process and develop innovative treatment methods for IMI toxicity [13].

Many studies have established a link between ER stress and NLRP3-mediated pyroptosis in the development of pancreatic damage. If research can develop a method to alleviate this effect, it may serve as a therapeutic approach to reduce IMI-induced pancreatic damage [14].

Lycopene, a non-provitamin A carotenoid, is abundant in the human diet. It is not synthesized by the body and can only be obtained through dietary consumption [15]. According to Milani et al., lycopene exhibits antioxidant properties by scavenging O<sub>2</sub> and OH<sup>-</sup>, thereby reducing the risk of oxidative stress-related chronic illnesses such as cancer, hypertension, cardiovascular disease, and pancreatic disorders [16,17]. Furthermore, it inhibits oxidative stress and inflammation by suppressing the NF-κB pathway [18]. However, its protective effect on the pancreas against IMI has not been studied extensively.

This study aims to elucidate the protective effects of lycopene on various cellular activities and signalling pathways, as well as to investigate its interaction with the pathogenesis of IMI-induced pancreatic dysfunction and to review the literature.

## 2. Materials and Methods

### 2.1. Drugs and Chemicals

Imidacloprid (IMI) [1-(6-chloro-3-pyridylmethyl)-N-nitroimidazolidin-2-ylideneamine] [CAS No.138261-41-3] was obtained from BAYER company, Leverkusen, Germany. Lycopene (LYC) (C<sub>40</sub>H<sub>56</sub>; deep red powder CAS Number 502-65-8, purity > 95%) was obtained from Sigma-aldrich, St. Louis, MO, USA.

### 2.2. Animals and Ethics

Twenty-eight rats were utilized in this experiment. The general characteristics of the animals were as follows: (1) the rats were eight weeks old, (2) their weight ranged between 150 and 180 g ( $166.21 \pm 10.82$ ), and (3) they were male Sprague–Dawley rats. The rats were obtained from the animal house colony of the Faculty of Science, Benha University, Egypt. Throughout the entire experiment, the rats were divided into four groups and housed in well-ventilated cages at a room temperature of  $23 \pm 2$  °C, with a relative humidity of  $55 \pm 5\%$  and a 12 h light/dark cycle. The animals had ad libitum access to water as a source of food/fluid. The Research Ethics Committee of Benha University Faculty of Science (BUFS-REC-2023-34 Zoo) approved all animal interventions and conditions, complying with the Guidelines of the Laboratory Animals (NIH Publication No. 8023, revised).

### 2.3. Experimental Design

The rats were randomly assigned to four groups, each consisting of seven rats, as follows:

- Group I: Rats received 0.5 mL/day of corn oil, which served as the vehicle used in preparing IMI and LYC.
- Group II: Rats were treated with LYC dissolved in 0.5 mL corn oil at a dose of 10 mg/kg/day. Previous investigations have demonstrated that this dose is effective in producing antioxidant defence and reducing the toxicity of certain xenobiotics [19–24].
- Group III: Rats were treated with IMI at a dose of 45 mg/kg, which is 1/10 of the LD<sub>50</sub> [25–27].
- Group IV: Rats were treated with a combination of IMI (45 mg/kg) and LYC (10 mg/kg).

All drugs were administered orally on a daily basis for a duration of 30 days. Rats were put under anaesthesia using isoflurane. Using a cardiac puncture, blood samples were collected in plain sample bottles, and a laparotomy was conducted to obtain samples of pancreatic tissue. Blood samples were centrifuged ( $3000 \times g$  for a duration of 10 min) at room temperature, and the separated serum was used to analyse pancreatic enzymes and insulin levels. During the laparotomy, the pancreas was separated and dissected into three parts (head, body, and tail). The tail (the left lobe) was used for histopathological examination, the body part for inflammatory biomarker detection using a phosphate buffer saline, and the head (left lobe) of the specimen for RT-PCR mRNA quantification. Rats were euthanized via decapitation while under anaesthesia.

#### 2.4. Biochemical Parameters

##### 2.4.1. Evaluation of Amylase Activity, Insulin, and Glucose Levels

Quantitative determination of rat serum  $\alpha$ -amylase activity was performed utilizing a Vitro amylase reagent purchased from Vitro Scient, Belbis, Egypt. Enzymatic colorimetric determination of blood glucose (GOD-PAP methodology) was estimated using a Liqui CHEK glucose assay kit (AGAPPE. Diagnostic Ltd., Kerala, India). Serum insulin levels were assayed via a rat insulin ELISA kit (Cat. No. ERINS; Thermo Fisher Scientific, Waltham, MA, USA).

##### 2.4.2. Assessment of the Oxidative Stress Biomarkers and Inflammatory Mediators

A lipid peroxide (malondialdehyde) kit (Catalog # SD 25 29; BioDiagnostic, Giza, Egypt), a superoxide dismutase (SOD) kit (Catalog # SD 25 21; BioDiagnostic, Giza, Egypt), and a total antioxidant capacity (TAC) kit (Catalog # SD 25 13; BioDiagnostic, Giza, Egypt) were used to quantitatively detect the levels of malondialdehyde (MDA), SOD, and TAC, respectively, in the pancreatic tissue samples (colorimetric method). The Rat IL-1 $\beta$  Quantikine ELISA Kit (Catalog # RLB00) and Rat TNF- $\alpha$  Quantikine ELISA Kit (Catalog #: RTA00) purchased from R&D Systems, Minneapolis, MN, USA, were used to measure the levels of IL-1 $\beta$ , inflammatory mediators, and TNF- $\alpha$ .

#### 2.5. Real-Time Quantitative PCR (qPCR) Analysis for ATF6, CHOP, XBP1, IRE-1 $\alpha$ , BAX, and Casp-3 mRNA Expression

##### 2.5.1. RNA Purification and cDNA Synthesis

Trizol (Invitrogen; Thermo Fisher Scientific, Waltham, MA, USA.) was used to extract the total RNA from pancreatic tissue samples, and the A260/A280 ratio and quality of RNA were determined and analysed via a NanoDrop<sup>®</sup> ND-1000 Spectrophotometer (NanoDrop Technologies; Wilmington, DE, USA). Estimated RNA purity was between 1.8 and 2.0. For cDNA synthesis, a High-Capacity cDNA Reverse Transcription Kit cDNA Kit; (Applied Biosystems<sup>™</sup>, Thermo Fisher Scientific, Waltham, MA, USA) was used.

##### 2.5.2. mRNA Quantification

Real-time polymerase chain reaction (RT-PCR) was performed using a Mx3005P Real-Time PCR System (Agilent Stratagene, Santa Clara, CA, USA) and TOPreal<sup>™</sup> qPCR 2X PreMIX (SYBR Green with low ROX) obtained from Enzynomics, Daejeon, Korea. To initiate the PCR cycling conditions, the samples were initially denatured at 95 °C for 12 min, followed by 40 cycles of denaturation at 95 °C for 20 s, annealing at 60 °C for 30 s, and extension at 72 °C for 30 s. The oligonucleotide-specific primers were synthesized by Sangon Biotech (Beijing, China). The expression levels of the target gene were normalized using the mRNA expression of  $\beta$ -actin. The results were presented as fold changes using the  $2^{-\Delta\Delta CT}$  method [28] (Table 1).

**Table 1.** Primer sequences used in RT-PCR.

Gene	Forward Primer	Reverse Primer	Size	Accession No.
IRE-1 $\alpha$	GCGCAGGTGCAATGACATAC	CTCTTCCACGTGTGTTGGGA	178	NM_001191926.1
ATF6	AAGTGAAGAACCATTACTTTATATC	TTTCTGCTGGCTATTGT	157	NM_001107196.1
XBP1	TTACGAGAGAAAACATCATGGGC	GGGTCCAACCTGTCCAGAATGC	289	NM_001004210.2
CHOP	CACAAGCACCTCCCAAAG	CCTGCTCCTTCTCCTTCAT	158	NM_001109986.1
BAX	CGAATTGGCGATGAACTGGA	CAAACATGTCAGCTGCCACAC	109	NM_017059.2
Casp-3	GAGACAGACAGTGGAAGTACGATG	GGCGCAAAGTGACTGGATGA	147	NM_012922.2
act-b	AACCTTCTTGCAGCTCCTCC	CCATACCCACCATCACACCC	193	NM_031144.3

## 2.6. Histopathologic Study

Samples of pancreatic tissue were fixed in 10% neutral-buffered formalin for 72 h and then processed in serial upgrades of ethanol and subsequently cleared in xylene. Samples were then infiltrated and embedded into the Paraplast tissue embedding media. Sections approximately 5  $\mu$ m thick were sliced via a rotatory microtome to demonstrate the pancreatic parenchymal morphology following haematoxylin and eosin staining in accordance with the Bancroft and Layton 2018 protocol for routine histological examination [29].

One slide was prepared for each sample. Six representative non-overlapping fields were randomly selected and scanned from each sample by two histological professionals to study the histopathological changes.

### 2.6.1. Immunohistochemical Study

Approximately 5  $\mu$ m thick tissue sections were treated using 3% H<sub>2</sub>O<sub>2</sub> for 20 min, rinsed, and incubated using anti-insulin (bs-0056R—1:200—Bioss Co., Woburn, MA, USA), anti-NLRP3 (GTX00763—1:100—Genetex Co., Irvine, CA, USA), and anti-Caspase-1 antibody [NB100-56565—1:100—Novusbio Co., Centennial, CO, USA] at four degrees Celsius overnight. The sections were rinsed using PBS and incubated with a secondary antibody HRP Envision kit (DAKO) for 20 min. Sections were then incubated with diaminobenzidine (DAB) for 10 min following another wash also using PBS. The samples were washed for the last time, also using PBS, and then stained with haematoxylin, dehydrated, and cleared in xylene before being covered and slipped for examination. All standard procedures were carried out according to the standard protocol for routine histological examination [29].

### 2.6.2. IHC Analysis

One slide was prepared for each sample. Six representative non-overlapping fields were randomly selected and scanned per tissue section. The relative area percentage of positive reactions for Caspase 1, NLRP3, and anti-insulin in pancreatic islets (using the entire pancreatic parenchyma) was assessed as a standard module for IHC expressions. The true positive immune expression (indicated by brown colour) was identified in each field/tissue sample. All light microscopic examinations and data were collected using an automated-grade, standard-unit Leica Application module, which was pre-programmed for histological analysis. The module was connected to a Full HD microscopic imaging system (Leica Microsystems GmbH, Wetzlar, Germany) to analyse the total sample section based on the entire field area. Negative control staining was performed after exclusion of the primary antibody. The positive reaction was defined with a cytoplasmic brown colour.

Pancreatic tissue samples were sliced into small (1 mm<sup>3</sup>) pieces and fixed in 2.5% glutaraldehyde buffered to pH 7.4 with phosphate buffer for a duration of two hours. Using the same buffer, samples were washed and subsequently post-fixed via osmium tetroxide with phosphate buffer (1%) for two hours at room temperature. Using graded concentrations of ethanol, the tissue samples were dehydrated and embedded into Epon-Araldite resin. Samples were cut into ultrathin sections, then mounted on copper grids and double-stained with uranyl acetate followed by lead citrate. Using a transmission electron microscope (J.E.O.L., JEM-2100; Tokyo, Japan) operated at 80 kV, electron micrographs



were obtained, and this part of the experiment was performed at the electron Microscopic Unit, Faculty of Agriculture, Mansoura University, Mansoura, Egypt.

#### 2.6.3. Computer-Assisted Digital Image Analysis (Digital Morphometric Study)

EM images were acquired and analysed using VideoTest Morphology<sup>®</sup> software 5.2 on an Intel<sup>®</sup> Core I7<sup>®</sup>-based computer. The software facilitated the extraction of the following data: area measurements, colour intensity, and object counting. Granules were automatically identified and measured based on their colour difference, size, and circularity filter. The count and area measurements were performed with calibration to the image scale bar. The intensity of mitochondria was assessed through a semi-automated routine involving a combination of automatic selection and visual assessment. Six representative non-overlapping fields were randomly chosen and scanned. The selected areas were then subjected to an intensity measurement procedure.

#### 2.7. *In Silico* Study

Molecular docking was performed to assess the affinity of imidacloprid towards the Nrf2/Keap1 complex, PTEN for ROS/mitochondrial stress activation, and lycopene against the CHOP/IRE1- $\alpha$ /NLRP3 pathway. The target proteins (codes: 6QME, 5BZX, 1NWQ, 6XDB, and 7ALV) were obtained from the protein data bank. Initially, water molecules were removed from the complexes, and preparation options were utilized to correct crystallographic disorders and unfilled valence atoms. The protein structures were subjected to energy minimization using CHARMM force fields while preparing the pockets for the docking process. Using Chem-Bio Draw Ultra17.0, 2D structures of the tested compounds were drawn and saved as SDF files. The saved files were then opened, and the 3D structures were protonated. Energy minimization was carried out using the MMFF94 force field, aiming for a 0.1 RMSD kcal/mole energy. The minimized structures were prepared for docking using ligand preparation tools. The docking process was performed using MOE 2014 software [30]. The receptor was held rigid, while the ligands were allowed to be flexible. During refinement, each molecule generated twenty different poses with the proteins. The docking scores (affinity energy) of the best-fitted poses with the active sites were recorded, and 3D figures were generated using the Discovery Studio 2016 visualizer [31].

#### 2.8. Statistical Analysis

Data were collected in an Excel spreadsheet and analysed using SPSS version 22. The normality distribution was assessed using both the Kolmogorov–Smirnov test and the Shapiro–Wilk test. The Kruskal–Wallis test was applied to compare different groups. Data are represented as medians (IQR), and a significance level of 5% was considered. Box and whisker plots and line graphs were used to represent the data points. Line graphs were created using Microsoft Excel 365. Both principal component analysis (PCA) and the correlation matrix were conducted using GraphPad Prism software, version 9.5.1 (GraphPad Software, San Diego, CA, USA).

### 3. Results

Upon thorough examination, it was observed that the animals maintained normal body weight gain throughout the study, exhibiting regular feeding patterns and activity levels in all groups.

#### 3.1. Effect of LYC on Amylase Activity, Insulin, and Glucose Levels in IMI-Intoxicated Rats

As demonstrated in Figure 1, when tissues were exposed to toxic levels of IMI, this resulted in significantly ( $p < 0.05$ ) elevated plasma glucose and serum amylase levels compared to the LYC and normal control groups. Serum insulin levels were significantly decreased. The administration of LYC in IMI-intoxicated rats significantly reduced the